ACS chemical biology

Articles

pubs.acs.org/acschemicalbiology

An Orally Bioavailable Chemical Probe of the Lysine Methyltransferases EZH2 and EZH1

Kyle D. Konze,[†] Anqi Ma,[†] Fengling Li,[‡] Dalia Barsyte-Lovejoy,[‡] Trevor Parton,[§] Christopher J. MacNevin,[∥] Feng Liu,[†] Cen Gao,[†] Xi-Ping Huang,[⊥] Ekaterina Kuznetsova,[‡] Marie Rougie,[∥] Alice Jiang,[⊥] Samantha G. Pattenden,[†] Jacqueline L. Norris,[†] Lindsey I. James,[†] Bryan L. Roth,[⊥] Peter J. Brown,[‡] Stephen V. Frye,[†,¶] Cheryl H. Arrowsmith,[‡] Klaus M. Hahn,[∥,¶] Gang Greg Wang,[§,¶] Masoud Vedadi,[‡] and Jian Jin*[,†,¶]

[†]Center for Integrative Chemical Biology and Drug Discovery, Division of Chemical Biology and Medicinal Chemistry, UNC Eshelman School of Pharmacy, [§]Department of Biochemistry and Biophysics, School of Medicine, [∥]Department of Pharmacology, School of Medicine, [⊥]National Institute of Mental Health Psychoactive Drug Screening Program, and [¶]Lineberger Comprehensive Cancer Center, University of North Carolina at Chapel Hill, Chapel Hill, North Carolina 27599, United States

[‡]Structural Genomics Consortium, University of Toronto, Toronto, Ontario, M5G 1L7, Canada

Supporting Information

ABSTRACT: EZH2 or EZH1 is the catalytic subunit of the polycomb repressive complex 2 that catalyzes methylation of histone H3 lysine 27 (H3K27). The trimethylation of H3K27 (H3K27me3) is a transcriptionally repressive post-translational modification. Overexpression of EZH2 and hypertrimethylation of H3K27 have been implicated in a number of cancers. Several selective inhibitors of EZH2 have been reported recently. Herein we disclose UNC1999, the first orally bioavailable inhibitor that has high *in vitro* potency for wild-type and mutant EZH2 as well as EZH1, a closely related H3K27 methyltransferase that shares 96% sequence identity with EZH2 in their respective catalytic domains. UNC1999 was highly selective for EZH2 and EZH1 over a broad range of epigenetic and non-epigenetic targets, competitive with the cofactor SAM and non-competitive with the peptide substrate. This inhibitor potently reduced H3K27me3 levels in cells and selectively killed diffused large B cell lymphoma cell lines harboring the EZH2^{Y641N} mutant. Importantly, UNC1999 was orally bioavailable in mice, making this inhibitor a valuable tool for investigating the role of EZH2 and EZH1 in chronic animal studies. We also designed and synthesized UNC2400, a close analogue of UNC1999 with potency >1,000-fold lower than that of UNC1999 as a negative control for cell-based studies. Finally, we created a biotin-tagged UNC1999 (UNC2399), which enriched EZH2 in pull-down studies, and a UNC1999−dye conjugate (UNC2239) for co-localization studies with EZH2 in live cells. Taken together, these compounds represent a set of useful tools for the biomedical community to investigate the role of EZH2 and EZH1 in health and disease.

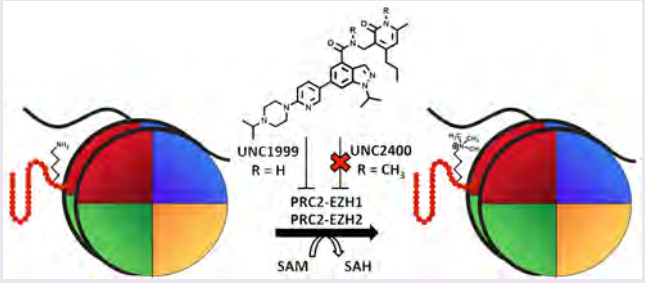

Among epigenetic "writers" (the enzymes that produce post-translational modifications (PTMs)), "readers" (the proteins that recognize and bind to PTMs), and "erasers" (the enzymes that remove PTMs), protein lysine methyltransferases (PKMTs, also known as histone methyltransferases (HMTs)), which catalyze mono-, di-, and/or trimethylation of lysine residues of histones and non-histone proteins, have increasingly been recognized as an important target class for modulation to regulate gene expression, cell differentiation, and organismal development.[1−12] Small-molecule probes[13] that selectively inhibit the catalytic activity of individual PKMTs are invaluable tools for deciphering the complex regulatory mechanisms enabled by histone and protein lysine methylation. Although the selective PKMT inhibitor discovery field is gaining momentum, only a limited number of selective inhibitors, which target the PKMT substrate binding groove,[14−20] cofactor binding site,[21−30] and a PRMT (protein arginine methyltransferase) allosteric binding site,[31,32] have been reported.

Polycomb repressive complex 2 (PRC2) that catalyzes methylation of histone H3 lysine 27 (H3K27) contains either the enzymatic subunit EZH2 (enhancer of zeste homologue 2, also known as KMT6 or KMT6A) or EZH1 (enhancer of zeste homologue 1, also known as KMT6B).[33−36] EZH2 and EZH1 are highly homologous and share 76% sequence identity overall and 96% sequence identity in their respective SET domains,[26] named after *Drosophila* Su(var.)3−9 (suppressor of variegation 3−9), E(z) (enhancer of zeste), and Trithorax.[37] Despite their high sequence identity, EZH2 and EZH1 are not functionally

Received: February 22, 2013
Accepted: April 8, 2013

   dx.doi.org/10.1021/cb400133j | *ACS Chem. Biol.* XXXX, XXX, XXX−XXX

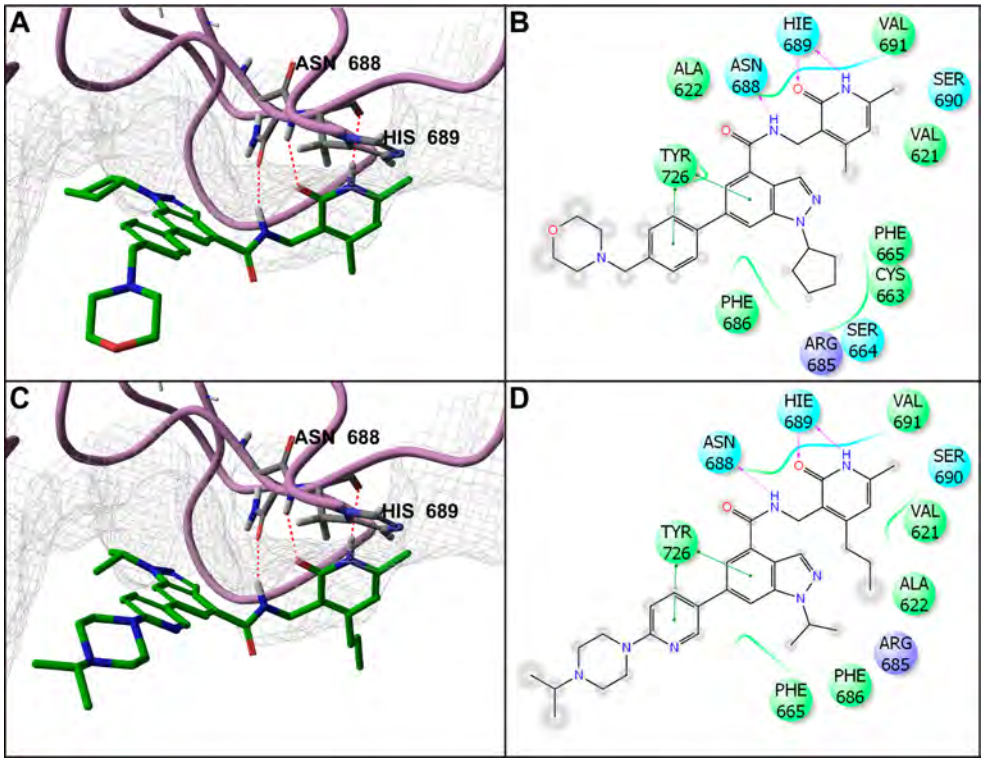

Figure 1. Binding hypothesis: UNC1999 binds to EZH2 similarly as EPZ005687, and its *N*-isopropyl piperazine moiety is solvent exposed. A homology model of EZH2 was constructed using GLP as a template (PDB: 2RFI). (A) EPZ005687 was docked into the SET domain; the ligand (green) orients such that the morpholine group is solvent exposed and therefore does not interact with EZH2 (purple). Additionally, there are three key hydrogen bonds that appear to be requisite for activity (dotted red lines). (B) Proposed ligand interactions of EPZ005687 display a hydrogen bond between the middle amide and Asn688 and two hydrogen bonds between the pyridone and His689 (purple arrows). (C) A docking model of UNC1999 shows it binds to EZH2 similarly as EPZ005687, and its *N*-isopropyl piperazine is solvent exposed. (D) Proposed ligand interactions of UNC1999 display the same key hydrogen bonds and hydrophobic interactions as EPZ005687.

redundant and have different expression patterns.[35,38] While EZH2 is found only in actively dividing cells, EZH1 is found in both dividing and non-dividing cells.[38] Although PRC2 containing EZH1 (PRC2−EZH1) has lower catalytic activity compared to that of PRC2 containing EZH2 (PRC2−EZH2), both complexes contribute to the maintenance of cellular H3K27 methylation states.[35,36,38]

The trimethylation of H3K27 (H3K27me3) catalyzed by PRC2 is a transcriptionally repressive epigenetic mark that regulates gene expression, differentiation, and development.[38] Dysregulation of EZH2, other PRC2 components, and H3K27 methylation has been associated with a number of cancers. For example, EZH2 is overexpressed in a broad spectrum of cancers including prostate, breast, myeloma, and lymphoma, and high expression correlates with poor prognosis.[38,39] More recently, hypertrimethylation of H3K27 has been identified in diffused large B cell lymphoma (DLBCL) cells heterozygous for point mutations recurrently targeting tyrosine 641 (Y641).[40,41] While wild-type (WT) EZH2 is most efficient at catalyzing monomethylation of non-methylated H3K27, the EZH2 Y641 mutant enzymes (Y641F, Y641N, Y641S, and Y641H) have the opposite substrate preference and are most efficient at catalyzing the conversion of dimethylated H3K27 (H3K27me2) into trimethylated H3K27 (H3K27me3).[40,41] Thus, the cooperation between WT and Y641 mutant EZH2 drives the hyper-trimethylation of H3K27 in these heterozygous DLBCL cells.[40,41] While targeting EZH2 dysfunction has been pursued as a potential therapeutic strategy for the treatment of cancer, it is worth noting that EZH2 and PRC2 play an integral part in regulating stem cell pluripotency and differentiation.[38,42] Therefore, developing an EZH2 chemical probe that has suitable pharmacokinetic (PK) properties would be extremely useful for assessing therapeutic benefit(s) and potential toxicity of chronically inhibiting EZH2 in animal studies.

The recent discoveries of EPZ005687, GSK126, and El1, the first potent and selective inhibitors of EZH2, were an important advance in the PKMT inhibitor discovery field.[24−26,28] These inhibitors share a common pyridone indazole/indole scaffold and are competitive with the cofactor *S*-adenosyl-L-methionine (SAM) and non-competitive with the peptide substrate. In cell-based studies, these inhibitors selectively reduced H3K27me3 and H3K27me2 marks and killed DLBCL cells bearing Y641 point mutations. However, EPZ005687 was reported to not have sufficient PK properties for animal studies, and *in vivo* PK properties of El1 were not reported. Although GSK126 was used in animal studies via intraperitoneal (IP) administration, no orally bioavailable EZH2 inhibitors that are more suitable for chronic animal studies have been reported to date. In addition, while EPZ005687, GSK126, and El1 are highly selective for EZH2 over other methyltransferases including EZH1, an inhibitor that has high *in vitro* potency and selectivity for both EZH2 and EZH1 over other methyltransferases has not been reported. Such a tool is expected to inhibit H3K27 methylation mediated by both PRC2−EZH2 and PRC2−EZH1 and, therefore, could offer potential advantages over EZH2 selective inhibitors in the disease settings where both PRC2−EZH2 and PRC2−EZH1 contribute to the methylation of H3K27.

dx.doi.org/10.1021/cb400133j | *ACS Chem. Biol.* XXXX, XXX, XXX−XXX

Table 1. *In Vitro* Potencies of Newly Synthesized Inhibitors

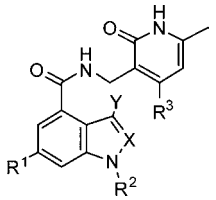

Compound	R^1	R^2	R^3	X	Y	EZH2 IC_{50} (nM)	clogP
1	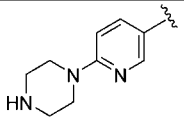		*n*-Pr	N	H	<10[a, b]	2.1
2	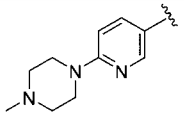		*n*-Pr	N	H	<10[a, b]	2.5
3	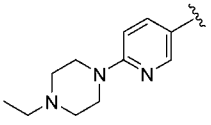		*n*-Pr	N	H	<10[a, b]	2.8
UNC1999 (**4**)	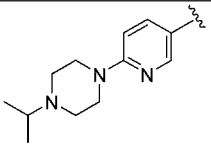		*n*-Pr	N	H	<10[a, b]	3.1
5	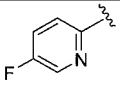		*n*-Pr	N	H	10 ± 1[a]	2.3
6	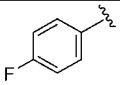		*n*-Pr	N	H	63 ± 2[a]	3.2
EPZ005687	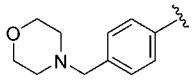		Me	N	H	54 ± 5[c]	2.2
GSK126	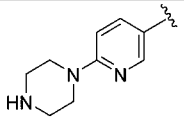		Me	CH	Me	10[c]	2.6

[a]IC_{50} determination experiments were performed in triplicate. [b]The IC_{50} limit of the EZH2 radioactive biochemical assay is 10 nM because the concentration of EZH2 used in this assay is 20 nM. [c]IC_{50} values obtained from refs 24 and 25, respectively.

Here we report the design, synthesis, and biological characterization of UNC1999, the first orally bioavailable chemical probe of EZH2 and EZH1. UNC1999 was highly potent and selective for EZH2 wild-type and Y641 mutant enzymes as well as EZH1 over a broad range of epigenetic and non-epigenetic targets. It was competitive with the cofactor and non-competitive with the peptide substrate. In cell-based assays, UNC1999 potently reduced the H3K27me3 mark and selectively killed DB cells, a DLBCL cell line harboring the $EZH2^{Y641N}$ mutant. In mouse PK studies, UNC1999 was orally bioavailable, making it suitable for chronic animal studies. We also report the discovery of UNC2400, which is a close analogue of UNC1999 with >1,000-fold less potency as a negative control for cellular studies, a biotinylated UNC1999 (UNC2399) that enriched EZH2 in pull-down studies, and a UNC1999–dye conjugate (UNC2239) for co-localization studies with EZH2 in live cells.

RESULTS AND DISCUSSION

Discovery of UNC1999 and UNC2400. To discover orally bioavailable EZH2 inhibitors, we docked EPZ005687 into an EZH2 homology model, which was built on the basis of the X-ray crystal structure of GLP (PDB: 2RFI), a H3K9 (histone H3

dx.doi.org/10.1021/cb400133j | *ACS Chem. Biol.* XXXX, XXX, XXX–XXX

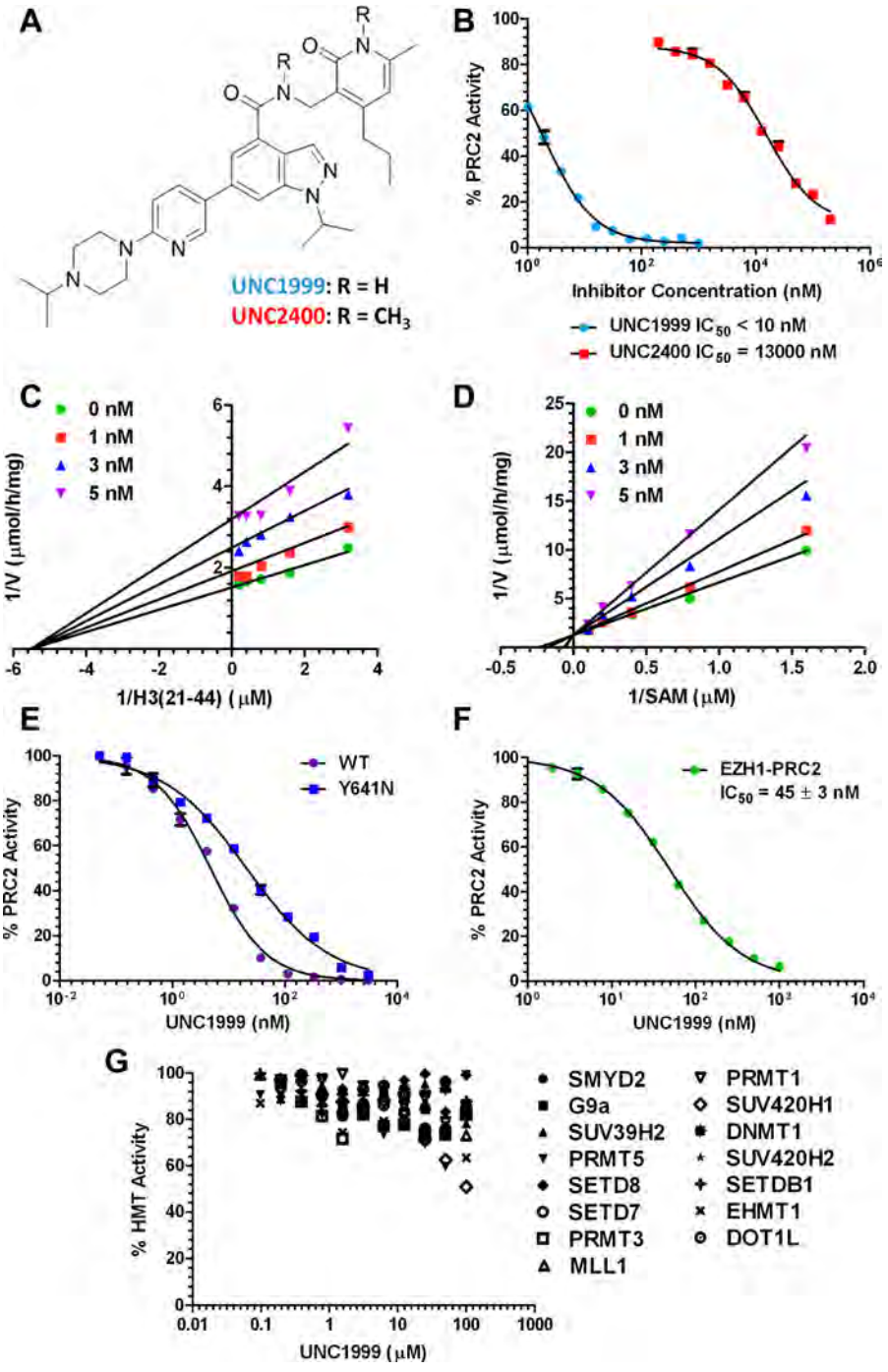

Figure 2. Characterization of UNC1999 and UNC2400 in biochemical assays. (A) Structure of UNC1999 and negative control UNC2400, which differs only by methylation at both amide nitrogens. (B) UNC2400 displays >1000-fold decrease in IC_{50} as compared to UNC1999 in the EZH2 radioactive assay. (C, D) Lineweaver−Burk plots demonstrate that UNC1999 is non-competitive with the histone H3 substrate (C) and competitive with the cofactor SAM (D). (E) UNC1999 is less than 5-fold more potent for WT EZH2 versus Y641N EZH2. (F) UNC1999 displays high potency (IC_{50} = 45 ± 3 nM) for EZH1. (G) UNC1999 is selective for EZH2 and EZH1 over 15 other lysine, arginine, and DNA methyltransferases.

lysine 9) mono- and dimethylase.[43] The docking model of EPZ005687 suggests that the morpholinomethyl moiety is solvent exposed and does not interact with EZH2. Other moieties of EPZ005687 make a number of hydrogen bonds and hydrophobic interactions with the EZH2 SAM binding site, including a hydrogen bond between the central amide and Asn688 (asparagine 688), and two hydrogen bonds between the pyridone and His689 (histidine 689) (Figure 1A and B). On the basis of this binding hypothesis, we designed multiple compounds that combine several key structural features of EPZ005687 and GSK126 (Figure 1C and D, and Table 1). We focused on modifying the morpholinomethyl region to modulate physicochemical properties of this series without disrupting protein−ligand interactions and kept the pyridone indazole core for maintaining key hydrogen bonds and hydrophobic interactions with the protein. Among these designed inhibitors, UNC1999 was docked into the EZH2 homology model. The docking model of UNC1999 suggests that (1) the secondary

dx.doi.org/10.1021/cb400133j | ACS Chem. Biol. XXXX, XXX, XXX−XXX

amide and pyridone maintain the respective key hydrogen bonds with Asn688 and His689, (2) the indazole is buried in a hydrophobic pocket, and (3) the *N*-isopropyl piperazine does not interact with the protein (Figure 1C and D). As expected, UNC1999 and EPZ005687 bind to the EZH2 SAM binding site very similarly according to these docking studies (Figure 1).

The compounds in Table 1 were synthesized (Supplementary Scheme S1) and evaluated in an EZH2 radioactive biochemical assay, which measures the transfer of the tritiated methyl group from the cofactor ^{3}H-SAM to a peptide substrate. IC_{50} values of these compounds in this assay and their calculated partition coefficient (clogP) values are summarized in Table 1. As expected, the unsubstituted and *N*-alkyl piperazines (compounds **1**−**4**) had high *in vitro* potency for EZH2 (IC_{50} < 10 nM), indicating that modifications to the *N*-capping group are well tolerated. These results support our binding hypothesis: the *N*-alkyl piperazine does not interact with the protein. Among these four inhibitors, UNC1999 (compound **4**) has a more desirable clogP (3.1).[44] This balanced lipophilicity could enhance oral absorption without a significant increase in metabolism. In addition, UNC1999 has a clogP higher than that of either EPZ005687 (2.2) or GSK126 (2.6), suggesting that UNC1999 may be better absorbed orally than either of the known inhibitors. Interestingly, replacing the 2-piperazinyl pyridin-5-yl moiety (compounds **1**−**4**) with a 3-fluoro pyridin-6-yl group (compound **5**) retained high *in vitro* potency (IC_{50} = 10 ± 1 nM (n = 3)). On the other hand, replacing the 3-fluoro pyridin-6-yl group (compound **5**) with a 4-fluorophenyl group (compound **6**) led to a 6-fold loss of potency. On the basis of these results, we selected UNC1999 for subsequent mechanism of action (MOA), selectivity, cellular assays, and mouse PK studies.

To provide the research community with a set of useful tools, we aimed to create a structurally similar but significantly less potent EZH2 inhibitor as a negative control for cell-based studies. On the basis of the UNC1999 docking model, which suggests that the secondary amide and pyridone form key hydrogen bonds with Asn688 and His689 (Figure 1C and D), we designed and synthesized UNC2400 (Figure 2A, Supplementary Scheme S2), which contains an *N*-methyl group at both the secondary amide and pyridone moieties of UNC1999. We hypothesized that the addition of these two *N*-methyl groups would abolish the hydrogen bond between the secondary amide and Asn688 and impair the hydrogen bonds between the pyridone and His689. Indeed, UNC2400 displayed an IC_{50} of 13,000 ± 3,000 nM (n = 3) in the EZH2 radioactive biochemical assay (Figure 2B), more than 1000-fold less potent than UNC1999, thus supporting our *in silico* binding hypothesis for UNC1999. Importantly, UNC2400 was also inactive in a number of cell-based studies (see below). The high structural similarity and drastic potency difference between UNC1999 and UNC2400 suggest they will be excellent positive and negative control tool compounds.

UNC1999 Is a SAM-Competitive, Potent, and Selective Inhibitor of EZH2 and EZH1. To determine the MOA of EZH2 inhibition by UNC1999, we generated classic Lineweaver−Burk plots[45] (Figure 2C and D), which indicate that UNC1999 was competitive with the cofactor SAM with a K_i of 4.6 ± 0.8 nM (n = 2) and non-competitive with the H3 peptide substrate. We also determined that increasing the H3 peptide concentration had no effect on the IC_{50} values of UNC1999, while increasing SAM concentration dramatically affected the IC_{50} values of UNC1999 (Supplementary Figure S1), which further supports that UNC1999 is a SAM-competitive EZH2 inhibitor. We next determined the potency of UNC1999 against EZH2 Y641 mutants. UNC1999 was highly potent for both Y641N and Y641F mutants (Figure 2E and Supplementary Figure S2), displaying less than 5-fold higher potency for the WT over the Y641N mutant enzyme and similar potencies for the WT and Y641F mutant enzymes.

To determine the selectivity profile of UNC1999, we first tested UNC1999 against EZH1. Compared with EPZ005687, GSK126 and El1, which are at least 50-fold selective for EZH2 over EZH1,[24,25,28] UNC1999 had high *in vitro* potency for EZH1 (IC_{50} = 45 ± 3 nM (n = 3)) (Figure 2F) and was only about 10-fold less potent for EZH1 than EZH2. We also determined the MOA of EZH1 inhibition by UNC1999 (Supplementary Figure S3). As indicated by the Lineweaver−Burk plots, UNC1999 was competitive with the cofactor SAM and non-competitive with the H3 peptide substrate. Because EZH1 and EZH2 are highly homologous and share 96% sequence identity in their respective SET domains,[26] it is not surprising that UNC1999 retains high *in vitro* potency for EZH1. However, it is not clear how the structural changes contribute to the switch from GSK126's high EZH2/EZH1 selectivity (>150-fold) to UNC1999's low EZH2/EZH1 selectivity (approximately 10-fold). The dual inhibition of EZH2 and EZH1 by UNC1999 might result in higher efficacy in cell-based and animal models where the methylation of H3K27 by PRC2−EZH2 is compensated for by PRC2−EZH1. This inhibitor may also be useful for assessing potential toxicities due to pharmacological inhibition of both EZH2 and EZH1. We next tested UNC1999 against 15 other lysine, arginine, or DNA methyltransferases (Figure 2G) and found that UNC1999 was more than 10,000-fold selective for EZH2 (IC_{50} < 10 nM) over these methyltransferases (IC_{50} > 100,000 nM).

We also evaluated the selectivity of UNC1999 over a broad range of non-epigenetic targets. Because UNC1999 was competitive with SAM, an adenine nucleoside, we tested it against a panel of 50 representative kinases (Supplementary Table S1). UNC1999 showed no appreciable inhibition (no more than 20% inhibition at 10,000 nM) against these kinases. In addition, we tested UNC1999 in the National Institute of Mental Health (NIMH) Psychoactive Drug Screen Program (PDSP) Selectivity Panel, which consists of a total of 44 GPCRs, transporters, and ion channels (Supplementary Table S2). It was found to show no more than 50% inhibition at 10,000 nM against 40 targets and >50% inhibition at 10,000 nM against 4 targets in the panel. K_i determinations in the radioligand binding assay for each of the 4 interacting targets was subsequently performed (Supplementary Table S3). UNC1999 had K_i values of 4,700 nM, 65 nM, 300 nM, and 1,500 nM for sigma1, sigma2, histamine H_3, and NET (norepinephrine transporter), respectively. Although we could not evaluate UNC1999 in sigma2 functional assays because they are unknown, we tested UNC1999 in histamine H_3 functional assays and found that it did not display any agonist or antagonist activities at concentrations up to 1,000 nM. Therefore, with the exception of sigma2, UNC1999 was more than 200-fold selective for EZH2 over a broad range of kinases, GPCRs, transporters, and ion channels.

In addition, we determined selectivity of UNC2400 versus other methyltransferases. As expected, UNC2400 displayed poor potencies for EZH1 (IC_{50} = 62,000 ± 7,000 nM (n = 3)) and EZH2 Y641F (IC_{50} > 200,000 nM) (Supplementary Figure S4A). It had negligible activity against 15 other methyltransferases (Supplementary Figure S4B)

UNC1999 Potently Reduces H3K27me3 in Cells. To assess the cellular potency of UNC1999, we employed an

dx.doi.org/10.1021/cb400133j | *ACS Chem. Biol.* XXXX, XXX, XXX−XXX

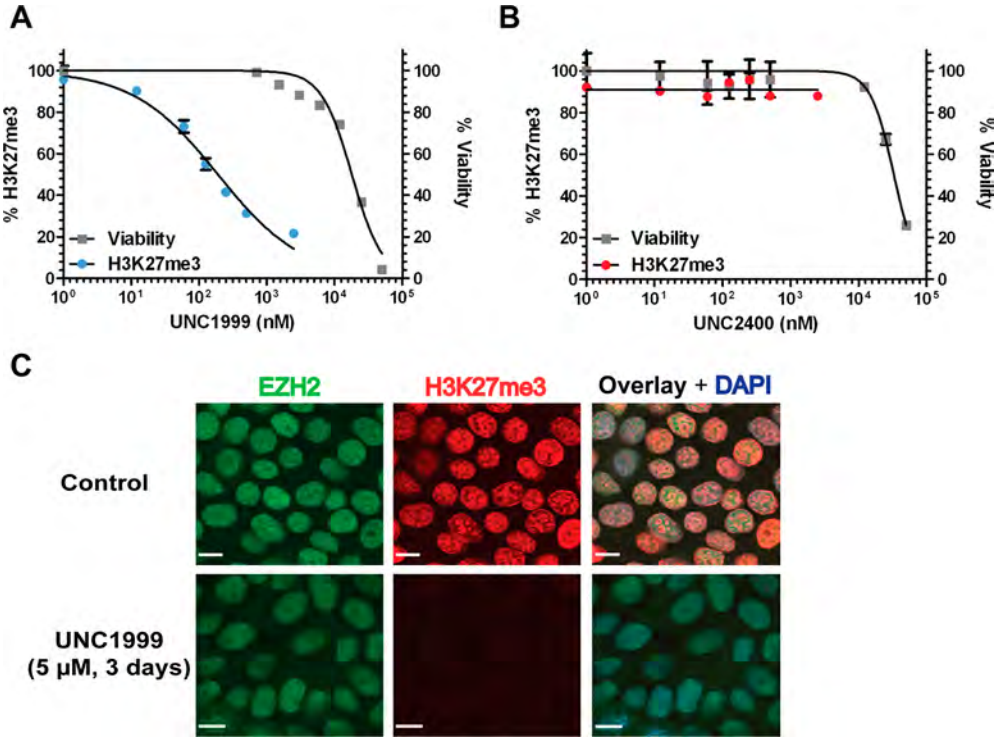

Figure 3. UNC1999 potently reduces H3K27me3 levels in cells and shows low cell toxicity. (A) UNC1999 reduces H3K27me3 levels in MCF10A cells with an IC_{50} = 124 ± 11 nM (n = 3) as determined by the ICW assay (blue) and displays low cell toxicity (EC_{50} = 19,200 ± 1200 nM (n = 3)) in the resazurin assay (gray). (B) UNC2400 displays negligible inhibition of H3K27me3 levels (red) in MCF10A cells while displaying toxicity (EC_{50} = 27,500 ± 1,300 (n = 3)) in the resazurin assay (gray) similar to that of UNC1999. (C) Immunofluorescence staining showed that treatment with UNC1999 (5 μM, 72 h) effectively reduced the H3K27me3 mark but did not affect EZH2 levels in MCF7 cells. Scale bar represents 10 μm.

H3K27me3 antibody cell immunofluorescence in-cell western (ICW) assay. This assay allows rapid processing of multiple samples for H3K27me3 immunofluorescence signal and normalization to cell number via the use of the nucleic acid dye DRAQ5. We characterized UNC1999 and UNC2400 in MCF10A cells, which bear the WT EZH2 enzyme. UNC1999 (72 h exposure) exhibited concentration-dependent reductions in H3K27me3 with an IC_{50} of 124 ± 11 nM (n = 3) (Figure 3A). On the other hand, UNC2400 (negative control) showed little or no activity in this ICW assay (Figure 3B), which is consistent with its poor *in vitro* potency. In addition, the treatment of MCF7 cells with UNC1999 at 5,000 nM for 72 h almost completely removed the H3K27me3 mark but did not have significant effects on cellular levels of EZH2 (Figure 3C).

One of the desirable characteristics of a high quality chemical probe is low toxicity due to off-target effects. Both UNC1999 (EC_{50} = 19,200 ± 1,200 nM (n = 3)) and UNC2400 (EC_{50} = 27,500 ± 1,300 (n = 3)) had low cellular toxicity in a standard resazurin (Alamar Blue) reduction assay (Figure 3A and B). Interestingly, UNC2400 showed similar cellular toxicity as UNC1999, suggesting that the observed low cellular toxicity is unlikely due to inhibition of EZH2 and EZH1 in this cell type. Taken together, UNC1999 had an excellent separation of cellular potency and toxicity with a function/toxicity ratio of more than 150 (Figure 3A).

UNC1999 Selectively Kills EZH2 Mutant DLBCL Cells. We next investigated whether DB cells, a DLBCL cell line harboring the $EZH2^{Y641N}$ mutant,[41,46] are more sensitive to UNC1999 treatment. UNC1999 (8 day exposure) displayed robust, concentration-dependent inhibition of cell proliferation with an EC_{50} of 633 ± 101 nM (n = 3) (Figure 4A), which is slightly more potent than GSK126.[25] At 5,000 nM, UNC1999 (8 day exposure) completely killed DB cells. Interestingly, we observed a delayed onset of activity for UNC1999: the 3 day

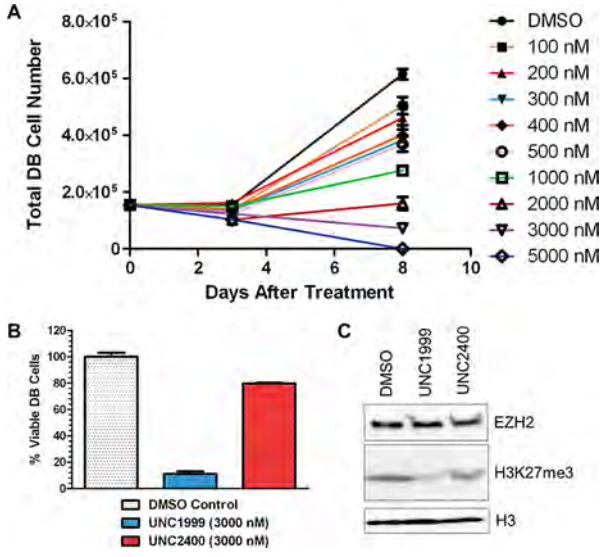

Figure 4. UNC1999 selectively kills DB cells, a DLBCL cell line with the EZH2 Y641N mutation. (A) UNC1999 displays a concentration- and time-dependent inhibition of DB cell proliferation (EC_{50} = 633 ± 101 nM (n = 3)). (B) UNC2400 (3000 nM, 8 days) does not significantly inhibit DB cell proliferation in contrast to UNC1999. (C) Western blotting of EZH2, H3K27me3, and H3 following the treatment of DB cells with UNC1999 or UNC2400 at 3000 nM for 3 days. UNC1999 decreases H3K27me3 but not EZH2 levels, while UNC2400 does not significantly reduce H3K27me3 or EZH2 levels in DB cells.

dx.doi.org/10.1021/cb400133j | *ACS Chem. Biol.* XXXX, XXX, XXX−XXX

treatment with this inhibitor did not have significant effects on cell proliferation at all tested concentrations (Figure 4A), as was also seen with EPZ005687 and GSK126.[24,25] We also compared the effects of the negative control UNC2400 on cell proliferation with UNC1999. While UNC1999 (3,000 nM, 8 day treatment) significantly inhibited DB cell proliferation, UNC2400 (3,000 nM, 8 day treatment) had negligible effects (Figure 4B). Furthermore, UNC1999 (3,000 nM, 3 day treatment) significantly reduced the H3K27me3 mark but did not significantly change EZH2 levels in DB cells (Figure 4C). On the other hand, treatment with UNC2400 at 3,000 nM for 3 days did not result in a significant reduction in the H3K27me3 mark nor EZH2 levels in DB cells (Figure 4C). Combining the observed low toxicity in MCF10A cells and high sensitivity in DB cells, we provide evidence that UNC1999 selectively kills DLBCL cells heterozygous for Y641 point mutations. In addition, we showed that UNC1999 has robust on-target activities in cells and that UNC2400 is an excellent negative control for cell-based studies.

UNC1999 Is Orally Bioavailable in Mice. We next evaluated the *in vivo* PK properties of UNC1999. A single intraperitoneal (IP) injection of UNC1999 at 15, 50, or 150 mg/kg achieved high C_{max} (9,700−11,800 nM) and exhibited dose linearity in male Swiss albino mice (Figure 5A). Both the 150 and

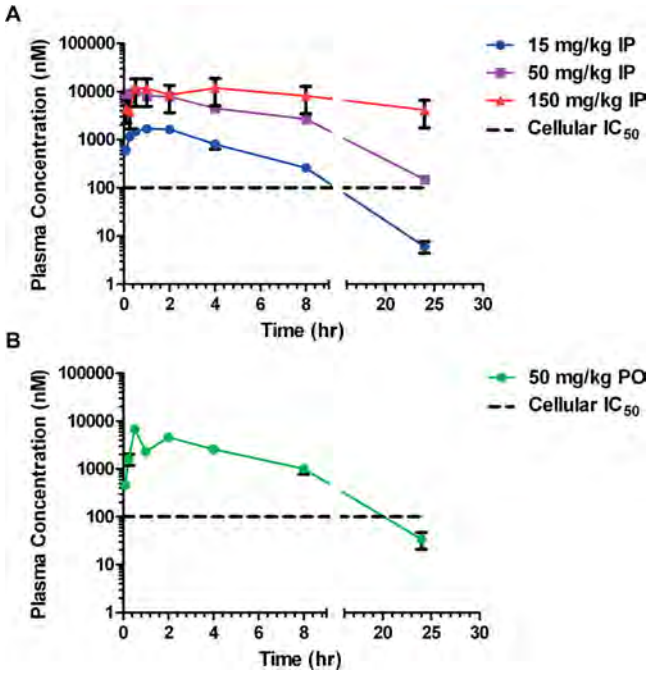

Figure 5. Pharmacokinetic profiles of UNC1999 in male Swiss albino mice. Plasma concentrations of UNC1999 following (A) a single IP injection (15, 50, or 150 mg/kg) or (B) a single oral dose (50 mg/kg) over the 24 h period. The dashed black line indicates the cellular IC_{50} of UNC1999.

50 mg/kg IP doses resulted in the plasma concentrations of UNC1999 above its cellular IC_{50} over the entire 24 h period, while the 15 mg/kg IP dose led to the plasma concentrations of UNC1999 above its cellular IC_{50} for approximately 12 h. We next examined whether UNC1999 is orally bioavailable and were pleased to find that a single 50 mg/kg oral dose of UNC1999 achieved high C_{max} (4,700 nM) and good exposure levels in male Swiss albino mice (Figure 5B). The plasma concentrations of UNC1999 were maintained above its cellular IC_{50} for approximately 20 h following this single oral dose. It is worth noting that all doses including the 150 mg/kg IP dose were well tolerated by all test mice, and no adverse effects were observed.

Compared with existing EZH2 inhibitors such as EPZ005687, which was reported to not have sufficient *in vivo* PK properties,[24,28] and GSK126, which was used only via IP injection,[25] UNC1999 is the first orally bioavailable inhibitor of EZH2 and EZH1. An orally bioavailable inhibitor makes chronic animal studies more practical and convenient as such a compound could be simply administered in the food or water of test mice. On the other hand, chronic daily IP injections to test mice could lead to infections, which might complicate long-term animal studies. Therefore, UNC1999 is a valuable tool for the biomedical research community to assess long-term therapeutic benefit(s) and potential toxicity resulting from pharmacological inhibition of EZH2 and EZH1 in mouse models.

Biotinylated UNC1999 Can Be Used To Pull Down EZH2 from Cell Lysates. Because the *N*-alkyl piperazine of UNC1999 is solvent exposed according to our docking model (Figure 1C and D) and modifications to the *N*-capping group were well tolerated (Table 1), we hypothesized that biotinylation at this site with a long PEG (poly(ethylene glycol)) linker would not disrupt key protein−ligand interactions. Thus, the resulting compound would retain high affinity to EZH2 and be useful for EZH2 pull-down studies. We therefore designed and synthesized UNC2399 (Figure 6A and Supplementary Scheme S3). Indeed, UNC2399 displayed high *in vitro* potency (IC_{50} = 17 ± 2 nM (n = 3)) in the EZH2 radioactive biochemical assay (Figure 6B). This result provides further evidence for our *in silico* binding hypothesis of UNC1999.

To conduct pull-down studies we first conjugated UNC2399 to streptavidin-coated beads. The compound-conjugated beads were used to capture EZH2 protein from HEK293T (human embryonic kidney 293T) cell lysates. We were pleased to find that UNC2399−streptavidin beads (Figure 6C, well 3) enriched EZH2 from cell lysates as compared to unconjugated streptavidin beads (DMSO control, Figure 6C, well 2). To control for nonspecific interactions, we pretreated the cell lysates with a soluble competitor, UNC1999 or UNC2400, before pull-down. As expected, the pretreatment with UNC1999 (100 μM) completely blocked the enrichment of EZH2 by UNC2399−streptavidin beads (Figure 6C, well 4 versus well 3). On the other hand, the pretreatment with UNC2400 (100 μM) resulted in EZH2 levels nearly identical to the samples that were not pretreated (Figure 6C, well 5 versus well 3). Taken together, these results provide evidence that UNC2399, a biotinylated UNC1999, is a useful tool for enriching EZH2 from cell lysates and lay the groundwork for future use of UNC2399 in chemoproteomics studies.

UNC1999−Dye Conjugate Co-localizes with EZH2 in Live Cells. We next sought to investigate the potential of UNC1999 to serve as a chemical probe for EZH2 localization in live cells. Based on the same principles used to design UNC2399, we designed UNC2239, which is a UNC1999−dye conjugate prepared by a click reaction between a UNC1999 analogue containing a terminal alkyne and a membrane permeant merocyanine dye with an azide side chain (Figure 7A and Supplementary Scheme S4). As expected, UNC2239 displayed high *in vitro* potency (IC_{50} = 21 ± 1 nM (n = 3)) in the EZH2 radioactive biochemical assay despite the addition of the fluorophore (Figure 7B).

Mouse embryonic fibroblast (MEF) cells stably expressing yellow fluorescent protein (YFP) were treated with the

dx.doi.org/10.1021/cb400133j | *ACS Chem. Biol.* XXXX, XXX, XXX−XXX

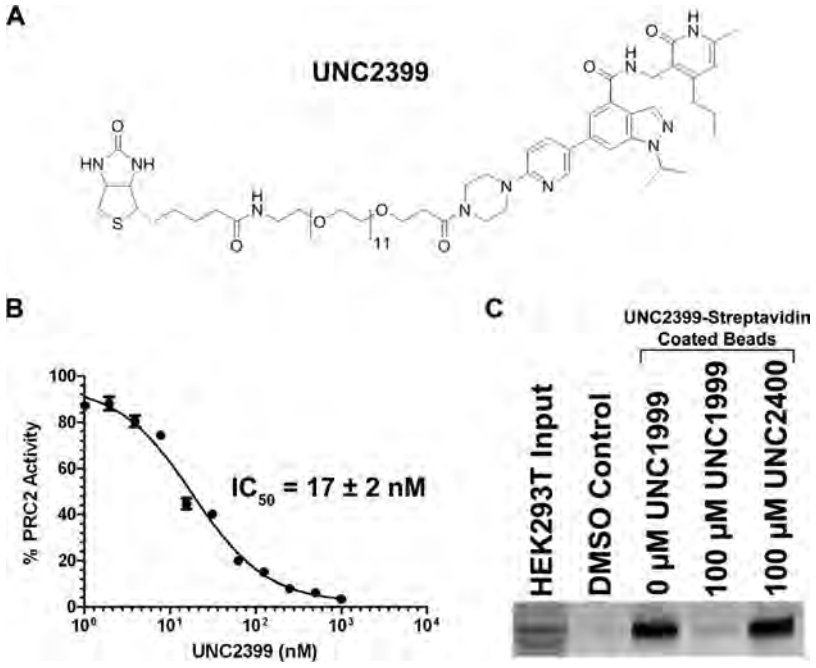

Figure 6. Biotinylated UNC1999 (UNC2399) enriches EZH2 from HEK293T cell lysates. (A) Structure of UNC2399, a biotinylated UNC1999. (B) UNC2399 displays high *in vitro* potency (IC_{50} = 17 ± 2 nM) for EZH2. (C) In UNC2399 pull-down experiments EZH2 levels are markedly enriched (well 3) as compared to the DMSO control (well 2). The ability to pull-down EZH2 out of cell lysates is abolished by pretreatment with 100 μM UNC1999 (well 4) but is not affected by pretreatment with 100 μM UNC2400 (well 5). This western blot is representative of three biological replicates.

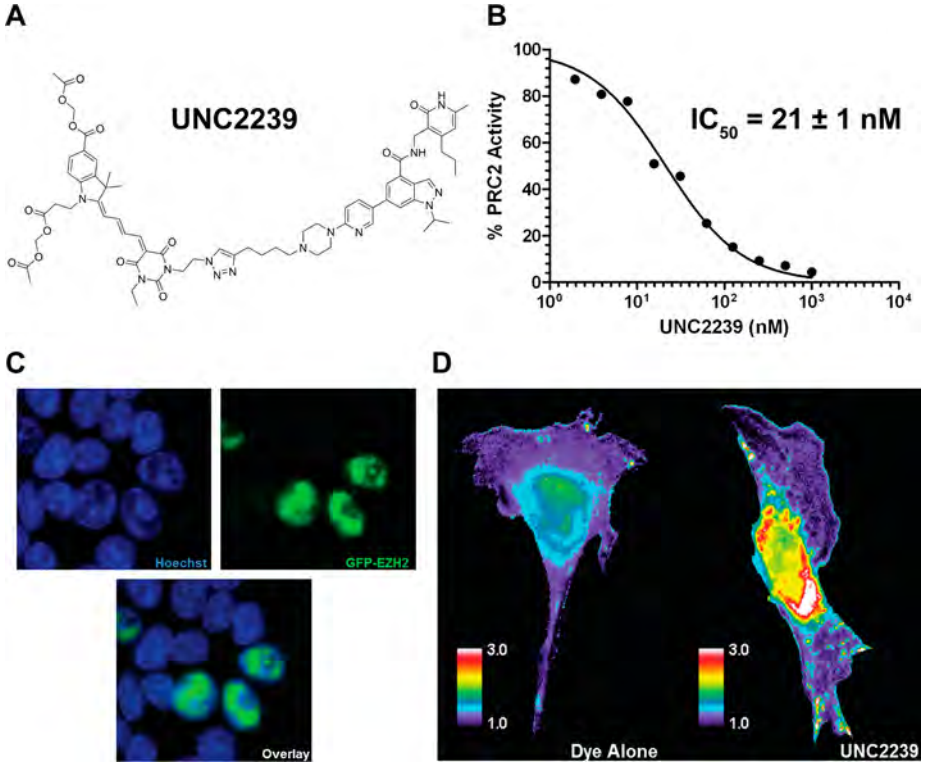

Figure 7. Live cell imaging with the fluorescent probe for EZH2. (A) Structure of UNC2239, a fluorescent dye conjugate of UNC1999. (B) UNC2239 displays high *in vitro* potency (IC_{50} = 21 ± 1 nM) for EZH2. (C) HEK293 cells transfected with EZH2-GFP and stained with nuclear marker Hoechst 33342 show nuclear localization of EZH2-GFP. (D) Ratio images showing localization of the EZH2 probe in MEF cells. The ratio of dye fluorescence intensity over YFP volume control fluorophore intensity was determined. Cells were normalized by setting the lowest 5% of cytoplasmic ratio values equal to 1. Cells treated with the EZH2 probe show greater fluorescence intensity in the nucleus than do cells treated with dye only.

fluorescent EZH2 probe UNC2239 or with the dye component of the probe only as a control (Figure 7D). The dye is known to distribute uniformly in MEF cells without evidence of any compartmental or organelle specific interactions. YFP serves as a uniformly distributed volume control fluorophore. When examining the localization of the probe, the ratio of dye intensity

dx.doi.org/10.1021/cb400133j | *ACS Chem. Biol.* XXXX, XXX, XXX−XXX

to YFP intensity was normalized for effects arising from varying cell thickness and uneven illumination intensity. Because the concentration of the probe and YFP varied from cell to cell, ratio images were normalized by setting the lowest 5% of pixels within each cell equal to 1. Cells treated with UNC2239 showed significantly higher fluorescence intensity in the nucleus relative to that in the cytoplasm compared to cells treated with the dye alone ($p < 0.05$, $n = 6$, Supplementary Figure S5). Perinuclear localization of the probe was also observed, potentially due to autophagocytic uptake of the probe. The observed localization of UNC2239 is consistent with the nuclear localization of GFP-tagged EZH2 as seen in transfected HEK 293 cells (Figure 7C), suggesting that UNC2239 co-localizes with EZH2.

Conclusions. We report the discovery of UNC1999, the first orally bioavailable chemical probe of EZH2 and EZH1. UNC1999 was highly potent and selective for EZH2 and EZH1 over a broad range of epigenetic and non-epigenetic targets and was competitive with the cofactor SAM and non-competitive with the peptide substrate. This inhibitor potently reduced the H3K27me3 mark in cells and selectively killed DB cells, a DLBCL cell line heterozygous with an $EZH2^{Y641N}$ mutant. Importantly, UNC1999 was orally bioavailable in mouse PK studies, thus making this inhibitor more suitable for assessing long-term therapeutic benefit(s) and potential toxicity of pharmacologically inhibiting EZH2 and EZH1 in animal studies than recently reported EZH2 inhibitors including EPZ005687 and GSK126. In addition, UNC1999 had high *in vitro* potency for both EZH2 and EZH1 while EPZ005687, GSK126, and El1 are more selective for EZH2 over EZH1. The dual inhibition of EZH2 and EZH1 by UNC1999 may offer potential advantages over EPZ005687, GSK126, and El1 in the disease settings where both PRC2−EZH2 and PRC2−EZH1 contribute to the methylation of H3K27. We also created UNC2400 which is a close analogue of UNC1999 with >1,000-fold lower potency than that of UNC1999 as a negative control for cellular studies, a biotinylated UNC1999 (UNC2399) that enriched EZH2 from cell lysates in pull-down studies, and a UNC1999−dye conjugate (UNC2239) for co-localization studies with EZH2 in live cells. Taken together, these valuable tools will aid in deciphering the role of EZH2 and EZH1 in health and disease.

METHODS

Synthesis of UNC1999 and Its Analogues. Synthetic schemes, experimental procedures, and full characterization data of all new compounds are described in Supporting Information.

In-Cell Western, Immunofluorescence Microscopy, and Cell Viability Assays. MCF10A cells were grown in DMEM/F12 media 5% horse serum, EGF (20 ng mL^{-1}), hydrocortisone (0.5 $\mu g\ mL^{-1}$), cholera toxin (100 ng mL^{-1}), and insulin (10 $\mu g\ mL^{-1}$) in the presence of inhibitors as stated in the figures. MCF7 cells were cultured in DMEM 10% FBS.

In-cell western fixation in 96-well black wall clear bottom plates was performed by 2% formaldehyde in PBS for 10 min. After five washes with 0.1% Triton X100 in PBS, cells were blocked for 1 h RT or overnight at 4 °C with 3% BSA, 5% goat serum in PBS. Three replicate wells from each experimental group were incubated in primary H3K27me3 antibody, Diagenode mAb-181-050 at 1/4000 dilution in 3% BSA, 5% goat serum PBS for 18 h at 4 °C. The wells were washed five times with 0.1% Tween 20 in PBS, then secondary IR800 conjugated antibody (Li-Cor) in Li-Cor blocking buffer (1:1000) and nucleic acid-intercalating dye, DRAQ5 (Cell Signaling Technologies) added for 1 h RT. After 5 washes with 0.1% Tween 20 PBS, the plates were read on an Odyssey (LiCor) scanner at 800 nm (H3K27me3 signal) and 700 nm (DRAQ5 signal). Fluorescence intensity was quantified, normalized to the background and then to the DRAQ5 signal, and expressed as a percentage of control.

Immunofluorescence microscopy was performed as above except the MCF7 cells were grown on the coverslips and stained for H3K27me3 (Diagenode) and EZH2 (Cell Signaling Technologies,) and secondary anti-mouse/rabbit antibodies used were conjugated to Alexa 488 and 555 (Cell Signaling Technologies). After washes with 0.1% Tween 20 PBS, the coverslips were mounted with DAPI Shield (Sigma) and analyzed on Zeiss spinning disc confocal microscope.

Cell viability assays were performed using 0.1 mg mL^{-1} of resazurin (Sigma) in the media. Resazurin reduction was monitored with 544 nm excitation, measuring fluorescence at 590 nm.

DB Cell Proliferation Assay. DB cells, a diffuse-large B-cell lymphoma cell line harboring the EZH2 Y641N mutation,[41,46] were obtained from ATCC and cultured in RPMI 1640 supplemented with 10% fetal bovine serum, antibiotics, and various concentrations of compounds (DMSO control, UNC1999, or UNC2400). The medium containing the test compound or control was refreshed every 3 days. The numbers of viable cells from at least three independent experiments were measured using TC20 automated cell counter system (Biorad). Total histones were prepared from cell nuclei using an acidic extraction protocol as previously described.[47] About 1 μg of total histones was separated using 15% SDS-PAGE, transferred to PVDF membranes, and probed with histone antibodies. Antibodies used in this study are those against EZH2 (BD bioscience 612666), general H3 (Abcam ab1791), and H3K27me3 (Abcam ab6002).

UNC2399 Pull-Down Studies. HEK293T cells were grown in DMEM (Sigma) supplemented with 10% FBS. Approximately 1×10^6 cells were lysed using 500 μL of Cytobuster (Novagen) supplemented with 1X protease inhibitor cocktail (Roche no. 05056489001) and 125 U of Benzonase Nuclease (Novagen no. D00128165). Protein concentration was quantified using a Bradford assay (BioRad no. 500-0006), and then 1 mg of lysate was used for each pull-down. Bead conjugates were prepared by incubating 0.1 mM UNC2399 with 200 μg of Dynabeads Streptavidin-coated magnetic beads (Invitrogen no. 653.06) at RT with for 1 h. The beads were then washed 3 times with TBST (20 mM Tris-HCl, pH 8.0/150 mM NaCl/0.1% Tween-20) to remove excess unbound UNC2399. Unconjugated control and compound-conjugated beads were incubated with cell lysate on an end-over-end rotator at 4 °C overnight. Beads were washed 3 times with Wash Buffer (10 mM HEPES, pH7.9/0.2% Triton-X-100/0.3 M NaCl/10 mM KCl/1.5 mM $MgCl_2$), resuspended in 1X sample buffer (Invitrogen no. LC2676), and incubated at 95 °C for 5 min. Each sample was then run on a Mini-PROTEAN TGX gradient gel (BioRad no. 456-9035) followed by western blotting. Blots were blocked in 5% milk for 1 h, incubated with anti-EZH2 antibody (Abcam no. ab110646) overnight at 4 °C, washed 3 × 5 min with PBS/0.1% Tween-20, incubated 1 h with HRP-conjugated secondary (Jackson ImmunResearch Laboratories no. 211-032-171), washed as before, and then developed using ECL2 western blotting substrate (Pierce no. 80196). Imaging was performed on the Typhoon Trio+ (GE) imaging system. In the case of competitive experiments with free soluble UNC1999 or UNC2400, the lysate was incubated with compound for 1 h at RT before being introduced to the beads.

EZH2 Homology Modeling, Radioactive Biochemical Assays, Mechanism of Action Studies, Selectivity Assays, Mouse PK Studies, and UNC2239 Imaging Studies. Full experimental protocols are described in Supporting Information.

ASSOCIATED CONTENT

Supporting Information

This material is available free of charge via the Internet at http://pubs.acs.org.

AUTHOR INFORMATION

Corresponding Author

*E-mail: jianjin@unc.edu.

Notes

The authors declare no competing financial interest.

■ ACKNOWLEDGMENTS

We thank Wenhwa Lee for graphical design and illustration and the University Cancer Research Fund and Carolina Partnership from University of North Carolina at Chapel Hill and the V Foundation for Cancer Research for financial support. The Structural Genomics Consortium is a registered charity (number 1097737) that receives funds from the Canada Foundation for Innovation, Eli Lilly Canada, GlaxoSmithKline, the Ontario Ministry of Economic Development and Innovation, the Novartis Research Foundation, Pfizer, AbbVie, Takeda, Janssen, Boehringer Ingelheim, and the Wellcome Trust. This project was also funded by Genome Canada through the Ontario Genomics Institute per research agreement OGI-055. G.G.W. is supported by NIH/NCI "Pathway to Independence" Award in Cancer Research (R00CA151683) and a Junior Scholar award of the V Foundation for Cancer Research. This research was also supported by funding from the American Cancer Society (C.J.M., 119169-PF-10-183-01-TBE) and the National Institutes of Health (K.M.H., GM057464 and GM094663).

■ REFERENCES

(1) Arrowsmith, C. H., Bountra, C., Fish, P. V., Lee, K., and Schapira, M. (2012) Epigenetic protein families: a new frontier for drug discovery. *Nat. Rev. Drug Discovery 11*, 384−400.

(2) Copeland, R. A., Solomon, M. E., and Richon, V. M. (2009) Protein methyltransferases as a target class for drug discovery. *Nat. Rev. Drug Discovery 8*, 724−732.

(3) Kouzarides, T. (2007) Chromatin modifications and their function. *Cell 128*, 693−705.

(4) Martin, C., and Zhang, Y. (2005) The diverse functions of histone lysine methylation. *Nat. Rev. Mol. Cell. Biol. 6*, 838−849.

(5) Jenuwein, T., and Allis, C. D. (2001) Translating the histone code. *Science 293*, 1074−1080.

(6) Bernstein, B. E., Meissner, A., and Lander, E. S. (2007) The mammalian epigenome. *Cell 128*, 669−681.

(7) Gelato, K. A., and Fischle, W. (2008) Role of histone modifications in defining chromatin structure and function. *Biol. Chem. 389*, 353−363.

(8) Strahl, B. D., and Allis, C. D. (2000) The language of covalent histone modifications. *Nature 403*, 41−45.

(9) Huang, J., Perez-Burgos, L., Placek, B. J., Sengupta, R., Richter, M., Dorsey, J. A., Kubicek, S., Opravil, S., Jenuwein, T., and Berger, S. L. (2006) Repression of p53 activity by Smyd2-mediated methylation. *Nature 444*, 629−632.

(10) Huang, J., Dorsey, J., Chuikov, S., Zhang, X., Jenuwein, T., Reinberg, D., and Berger, S. L. (2010) G9A and GLP methylate lysine 373 in the tumor suppressor p53. *J. Biol. Chem. 285*, 9636−9641.

(11) Rathert, P., Dhayalan, A., Murakami, M., Zhang, X., Tamas, R., Jurkowska, R., Komatsu, Y., Shinkai, Y., Cheng, X., and Jeltsch, A. (2008) Protein lysine methyltransferase G9a acts on non-histone targets. *Nat. Chem. Biol. 4*, 344−346.

(12) Huang, J., Sengupta, R., Espejo, A. B., Lee, M. G., Dorsey, J. A., Richter, M., Opravil, S., Shiekhattar, R., Bedford, M. T., Jenuwein, T., and Berger, S. L. (2007) p53 is regulated by the lysine demethylase LSD1. *Nature 449*, 105−108.

(13) Frye, S. V. (2010) The art of the chemical probe. *Nat. Chem. Biol. 6*, 159−161.

(14) Kubicek, S., O'Sullivan, R. J., August, E. M., Hickey, E. R., Zhang, Q., Teodoro, M. L., Rea, S., Mechtler, K., Kowalski, J. A., Homon, C. A., Kelly, T. A., and Jenuwein, T. (2007) Reversal of H3K9me2 by a small-molecule inhibitor for the G9a histone methyltransferase. *Mol. Cell 25*, 473−481.

(15) Liu, F., Chen, X., Allali-Hassani, A., Quinn, A. M., Wasney, G. A., Dong, A., Barsyte, D., Kozieradzki, I., Senisterra, G., Chau, I., Siarheyeva, A., Kireev, D. B., Jadhav, A., Herold, J. M., Frye, S. V., Arrowsmith, C. H., Brown, P. J., Simeonov, A., Vedadi, M., and Jin, J. (2009) Discovery of a 2,4-diamino-7-aminoalkoxyquinazoline as a potent and selective inhibitor of histone lysine methyltransferase G9a. *J. Med. Chem. 52*, 7950−7953.

(16) Chang, Y., Ganesh, T., Horton, J. R., Spannhoff, A., Liu, J., Sun, A., Zhang, X., Bedford, M. T., Shinkai, Y., Snyder, J. P., and Cheng, X. (2010) Adding a lysine mimic in the design of potent inhibitors of histone lysine methyltransferases. *J. Mol. Biol. 400*, 1−7.

(17) Liu, F., Chen, X., Allali-Hassani, A., Quinn, A. M., Wigle, T. J., Wasney, G. A., Dong, A., Senisterra, G., Chau, I., Siarheyeva, A., Norris, J. L., Kireev, D. B., Jadhav, A., Herold, J. M., Janzen, W. P., Arrowsmith, C. H., Frye, S. V., Brown, P. J., Simeonov, A., Vedadi, M., and Jin, J. (2010) Protein lysine methyltransferase G9a inhibitors: Design, synthesis, and structure activity relationships of 2,4-diamino-7-aminoalkoxy-quinazolines. *J. Med. Chem. 53*, 5844−5857.

(18) Vedadi, M., Barsyte-Lovejoy, D., Liu, F., Rival-Gervier, S., Allali-Hassani, A., Labrie, V., Wigle, T. J., DiMaggio, P. A., Wasney, G. A., Siarheyeva, A., Dong, A., Tempel, W., Wang, S.-C., Chen, X., Chau, I., Mangano, T., Huang, X.-P., Simpson, C. D., Pattenden, S. G., Norris, J. L., Kireev, D. B., Tripathy, A., Edwards, A., Roth, B. L., Janzen, W. P., Garcia, B. A., Petronis, A., Ellis, J., Brown, P. J., Frye, S. V., Arrowsmith, C. H., and Jin, J. (2011) A chemical probe selectively inhibits G9a and GLP methyltransferase activity in cells. *Nat. Chem. Biol. 7*, 566−574.

(19) Liu, F., Barsyte-Lovejoy, D., Allali-Hassani, A., He, Y., Herold, J. M., Chen, X., Yates, C. M., Frye, S. V., Brown, P. J., Huang, J., Vedadi, M., Arrowsmith, C. H., and Jin, J. (2011) Optimization of cellular activity of G9a inhibitors 7-aminoalkoxy-quinazolines. *J. Med. Chem. 54*, 6139−6150.

(20) Ferguson, A. D., Larsen, N. A., Howard, T., Pollard, H., Green, I., Grande, C., Cheung, T., Garcia-Arenas, R., Cowen, S., Wu, J., Godin, R., Chen, H., and Keen, N. (2011) Structural basis of substrate methylation and inhibition of SMYD2. *Structure 19*, 1262−1273.

(21) Daigle, S. R., Olhava, E. J., Therkelsen, C. A., Majer, C. R., Sneeringer, C. J., Song, J., Johnston, L. D., Scott, M. P., Smith, J. J., Xiao, Y., Jin, L., Kuntz, K. W., Chesworth, R., Moyer, M. P., Bernt, K. M., Tseng, J. C., Kung, A. L., Armstrong, S. A., Copeland, R. A., Richon, V. M., and Pollock, R. M. (2011) Selective killing of mixed lineage leukemia cells by a potent small-molecule DOT1L inhibitor. *Cancer Cell 20*, 53−65.

(22) Yao, Y., Chen, P., Diao, J., Cheng, G., Deng, L., Anglin, J. L., Prasad, B. V. V, and Song, Y. (2011) Selective inhibitors of histone methyltransferase DOT1L: Design, synthesis and crystallographic studies. *J. Am. Chem. Soc. 133*, 16746−16749.

(23) Yuan, Y., Wang, Q., Paulk, J., Kubicek, S., Kemp, M. M., Adams, D. J., Shamji, A. F., Wagner, B. K., and Schreiber, S. L. (2012) A small-molecule probe of the histone methyltransferase G9a induces cellular senescence in pancreatic adenocarcinoma. *ACS Chem. Biol. 7*, 1152−1157.

(24) Knutson, S. K., Wigle, T. J., Warholic, N. M., Sneeringer, C. J., Allain, C. J., Klaus, C. R., Sacks, J. D., Raimondi, A., Majer, C. R., Song, J., Scott, M. P., Jin, L., Smith, J. J., Olhava, E. J., Chesworth, R., Moyer, M. P., Richon, V. M., Copeland, R. A., Keilhack, H., Pollock, R. M., and Kuntz, K. W. (2012) A selective inhibitor of EZH2 blocks H3K27 methylation and kills mutant lymphoma cells. *Nat. Chem. Biol. 8*, 890−896.

(25) McCabe, M. T., Ott, H. M., Ganji, G., Korenchuk, S., Thompson, C., Van Aller, G. S., Liu, Y., Graves, A. P., Iii, A. D., Diaz, E., Lafrance, L. V., Mellinger, M., Duquenne, C., Tian, X., Kruger, R. G., McHugh, C. F., Brandt, M., Miller, W. H., Dhanak, D., Verma, S. K., Tummino, P. J., and Creasy, C. L. (2012) EZH2 inhibition as a therapeutic strategy for lymphoma with EZH2-activating mutations. *Nature 492*, 108−112.

(26) Verma, S. K., Tian, X., LaFrance, L. V., Duquenne, C., Suarez, D. P., Newlander, K. A., Romeril, S. P., Burgess, J. L., Grant, S. W., Brackley, J. A., Graves, A. P., Scherzer, D. A., Shu, A., Thompson, C., Ott, H. M., Aller, G. S. V., Machutta, C. A., Diaz, E., Jiang, Y., Johnson, N. W., Knight, S. D., Kruger, R. G., McCabe, M. T., Dhanak, D., Tummino, P. J., Creasy, C. L., and Miller, W. H. (2012) Identification of potent,

selective, cell-active inhibitors of the histone lysine methyltransferase EZH2. *ACS Med. Chem. Lett. 3*, 1091−1096.
(27) Zheng, W., Ibáñez, G., Wu, H., Blum, G., Zeng, H., Dong, A., Li, F., Hajian, T., Allali-Hassani, A., Amaya, M. F., Siarheyeva, A., Yu, W., Brown, P. J., Schapira, M., Vedadi, M., Min, J., and Luo, M. (2012) Sinefungin derivatives as inhibitors and structure probes of protein lysine methyltransferase SETD2. *J. Am. Chem. Soc. 134*, 18004−18014.
(28) Qi, W., Chan, H., Teng, L., Li, L., Chuai, S., Zhang, R., Zeng, J., Li, M., Fan, H., Lin, Y., Gu, J., Ardayfio, O., Zhang, J.-H., Yan, X., Fang, J., Mi, Y., Zhang, M., Zhou, T., Feng, G., Chen, Z., Li, G., Yang, T., Zhao, K., Liu, X., Yu, Z., Lu, C. X., Atadja, P., and Li, E. (2012) Selective inhibition of Ezh2 by a small molecule inhibitor blocks tumor cells proliferation. *Proc. Natl. Acad. Sci. U.S.A. 109*, 21360−21365.
(29) Yu, W., Chory, E. J., Wernimont, A. K., Tempel, W., Scopton, A., Federation, A., Marineau, J. J., Qi, J., Barsyte-Lovejoy, D., Yi, J., Marcellus, R., Iacob, R. E., Engen, J. R., Griffin, C., Aman, A., Wienholds, E., Li, F., Pineda, J., Estiu, G., Shatseva, T., Hajian, T., Al-awar, R., Dick, J. E., Vedadi, M., Brown, P. J., Arrowsmith, C. H., Bradner, J. E., and Schapira, M. (2012) Catalytic site remodelling of the DOT1L methyltransferase by selective inhibitors. *Nat. Commun. 3*, 1288.
(30) Williams, D. E., Dalisay, D. S., Li, F., Amphlett, J., Maneerat, W., Chavez, M. A. G., Wang, Y. A., Matainaho, T., Yu, W., Brown, P. J., Arrowsmith, C. H., Vedadi, M., and Andersen, R. J. (2013) Nahuoic acid A produced by a Streptomyces sp. isolated from a marine sediment is a selective SAM-competitive inhibitor of the histone methyltransferase SETD8. *Org. Lett. 15*, 414−417.
(31) Siarheyeva, A., Senisterra, G., Allali-Hassani, A., Dong, A., Dobrovetsky, E., Wasney, Gregory A., Chau, I., Marcellus, R., Hajian, T., Liu, F., Korboukh, I., Smil, D., Bolshan, Y., Min, J., Wu, H., Zeng, H., Loppnau, P., Poda, G., Griffin, C., Aman, A., Brown, P. J., Jin, J., Al-awar, R., Arrowsmith, C. H., Schapira, M., and Vedadi, M. (2012) An allosteric inhibitor of protein arginine methyltransferase 3. *Structure 20*, 1425−1435.
(32) Liu, F., Li, F., Ma, A., Dobrovetsky, E., Dong, A., Gao, C., Korboukh, I., Liu, J., Smil, D., Brown, P. J., Frye, S. V., Arrowsmith, C. H., Schapira, M., Vedadi, M., and Jin, J. (2013) Exploiting an allosteric binding site of PRMT3 yields potent and selective inhibitors. *J. Med. Chem. 56*, 2110−2124.
(33) Cao, R., Wang, L., Wang, H., Xia, L., Erdjument-Bromage, H., Tempst, P., Jones, R. S., and Zhang, Y. (2002) Role of histone H3 lysine 27 methylation in Polycomb-group silencing. *Science 298*, 1039−1043.
(34) Kuzmichev, A., Nishioka, K., Erdjument-Bromage, H., Tempst, P., and Reinberg, D. (2002) Histone methyltransferase activity associated with a human multiprotein complex containing the Enhancer of Zeste protein. *Genes Dev. 16*, 2893−2905.
(35) Shen, X., Liu, Y., Hsu, Y.-J., Fujiwara, Y., Kim, J., Mao, X., Yuan, G.-C., and Orkin, S. H. (2008) EZH1 mediates methylation on histone H3 lysine 27 and complements EZH2 in maintaining stem cell identity and executing pluripotency. *Mol. Cell 32*, 491−502.
(36) Margueron, R., Li, G., Sarma, K., Blais, A., Zavadil, J., Woodcock, C. L., Dynlacht, B. D., and Reinberg, D. (2008) Ezh1 and Ezh2 maintain repressive chromatin through different mechanisms. *Mol. Cell 32*, 503−518.
(37) Fog, C. K., Jensen, K. T., and Lund, A. H. (2007) Chromatin-modifying proteins in cancer. *Acta Pathol., Microbiol. Immunol. Scand. 115*, 1060−1089.
(38) Margueron, R., and Reinberg, D. (2011) The Polycomb complex PRC2 and its mark in life. *Nature 469*, 343−349.
(39) Simon, J. A., and Lange, C. A. (2008) Roles of the EZH2 histone methyltransferase in cancer epigenetics. *Mutat. Res. 647*, 21−29.
(40) Sneeringer, C. J., Scott, M. P., Kuntz, K. W., Knutson, S. K., Pollock, R. M., Richon, V. M., and Copeland, R. A. (2010) Coordinated activities of wild-type plus mutant EZH2 drive tumor-associated hypertrimethylation of lysine 27 on histone H3 (H3K27) in human B-cell lymphomas. *Proc. Natl. Acad. Sci. U.S.A. 107*, 20980−20985.
(41) Yap, D. B., Chu, J., Berg, T., Schapira, M., Cheng, S. W., Moradian, A., Morin, R. D., Mungall, A. J., Meissner, B., Boyle, M., Marquez, V. E., Marra, M. A., Gascoyne, R. D., Humphries, R. K., Arrowsmith, C. H., Morin, G. B., and Aparicio, S. A. (2011) Somatic mutations at EZH2 Y641 act dominantly through a mechanism of selectively altered PRC2 catalytic activity, to increase H3K27 trimethylation. *Blood 117*, 2451−2459.
(42) Chen, Y. H., Hung, M. C., and Li, L. Y. (2012) EZH2: a pivotal regulator in controlling cell differentiation. *Am. J. Trans. Res. 4*, 364−375.
(43) Tachibana, M., Ueda, J., Fukuda, M., Takeda, N., Ohta, T., Iwanari, H., Sakihama, T., Kodama, T., Hamakubo, T., and Shinkai, Y. (2005) Histone methyltransferases G9a and GLP form heteromeric complexes and are both crucial for methylation of euchromatin at H3-K9. *Genes Dev. 19*, 815−826.
(44) Lipinski, C. A., Lombardo, F., Dominy, B. W., and Feeney, P. J. (1997) Experimental and computational approaches to estimate solubility and permeability in drug discovery and development settings. *Adv. Drug Del. Rev. 23*, 3−25.
(45) Lineweaver, H., and Burk, D. (1934) The determination of enzyme dissociation constants. *J. Am. Chem. Soc. 56*, 658−666.
(46) Morin, R. D., Johnson, N. A., Severson, T. M., Mungall, A. J., An, J., Goya, R., Paul, J. E., Boyle, M., Woolcock, B. W., Kuchenbauer, F., Yap, D., Humphries, R. K., Griffith, O. L., Shah, S., Zhu, H., Kimbara, M., Shashkin, P., Charlot, J. F., Tcherpakov, M., Corbett, R., Tam, A., Varhol, R., Smailus, D., Moksa, M., Zhao, Y., Delaney, A., Qian, H., Birol, I., Schein, J., Moore, R., Holt, R., Horsman, D. E., Connors, J. M., Jones, S., Aparicio, S., Hirst, M., Gascoyne, R. D., and Marra, M. A. (2010) Somatic mutations altering EZH2 (Tyr641) in follicular and diffuse large B-cell lymphomas of germinal-center origin. *Nat. Genet. 42*, 181−185.
(47) Shechter, D., Dormann, H. L., Allis, C. D., and Hake, S. B. (2007) Extraction, purification and analysis of histones. *Nat. Protoc. 2*, 1445−1457.